Translational Oncology 42 (2024) 101867

Contents lists available at ScienceDirect

Translational Oncology

journal homepage: www.elsevier.com/locate/tranon

# Transforming growth factor-β1 and soluble co-inhibitory immune checkpoints as putative drivers of immune suppression in patients with basal cell carcinoma

Mahlatse C.M. Kgokolo [a,*], Nonkululeko Z. Malinga [a], Helen C. Steel [b], Pieter W.A. Meyer [b,c], Teresa Smit [d], Ronald Anderson [b], Bernardo L. Rapoport [b,d,*]

[a] Department of Dermatology, School of Medicine, Faculty of Health Sciences, University of Pretoria and Steve Biko Academic Hospital, Pretoria, South Africa
[b] Department of Immunology, School of Medicine, Faculty of Health Sciences, University of Pretoria, Pretoria, South Africa
[c] Tshwane Academic Division of the National Health Laboratory Service, Pretoria, South Africa
[d] The Medical Oncology Centre of Rosebank, Saxonwold, Johannesburg, South Africa

ARTICLE INFO

*Keywords:*
Arginase 1
Basal cell carcinoma
CTLA-4 antigen
PD-L1
Regulatory T-lymphocytes
Transforming growth factor-β1

ABSTRACT

The current study compared the levels and possible associations between systemic soluble immune checkpoints (sICPs, $n = 17$) and a group of humoral modulators of immune suppressor cells ($n = 7$) in a cohort of patients with basal cell carcinoma (BCC, $n = 40$) and a group of healthy control subjects ($n = 20$).

The seven humoral modulators of immunosuppressor cells were represented by the enzymes, arginase 1 and fibroblast activation protein (FAP), the chemokine, RANTES (CCL5) and the cytokines, interleukin-10 and transforming growth factor-β1 (TGF-β1), as well as the M2-type macrophage markers, soluble CD163 (sCD163) and sCD206.

The plasma levels of six co-inhibitory sICPs, sCTLA-4, sLAG-3, sPD-1, sPD-L1, sTIM-3 and sPD-L2 were significantly elevated in the cohort of BCC patients ($p<0.001$-$p<0.00001$), while that of sBTLA was significantly decreased ($p<0.006$). Of the co-stimulatory sICPs, sCD27 and sGITR were significantly increased ($p<0.0002$ and $p<0.0538$) in the cohort of BCC patients, while the others were essentially comparable with those of the control participants; of the dual active sICPs, sHVEM was significantly elevated ($p<0.00001$) and TLR2 comparable with the control group. A correlation heat map revealed selective, strong associations of TGF-β1 with seven co-stimulatory ($z = 0.618468$–$0.768131$) and four co-inhibitory ($z = 0.674040$–$0.808365$) sICPs, as well as with sTLR2 ($z = 0.696431$).

Notwithstanding the association of BCC with selective elevations in the levels of a large group of co-inhibitory sICPs, our novel findings also imply the probable involvement of TGF-β1 in driving immunosuppression in this malignancy, possibly via activation of regulatory T cells. Notably, these abnormalities were present in patients with either newly diagnosed or recurrent disease.

## Background

Basal cell carcinomas (BCCs) are common, low-grade, localized cutaneous malignancies of keratinocytic origin. They are amenable to eradication by surgical excision as the preferred first-line treatment, as well as by topical and systemic pharmacotherapy, radiotherapy, photodynamic and other therapies [1]. Notwithstanding excessive exposure to ultraviolet radiation, most prominently UVB, other immunosuppressive risk factors for development of BCCs, include genetic predisposition and iatrogenic- and age-related immune dysfunction. In the case of exposure of the skin to UVB, this results in excessive release of epidermal neuropeptides from neuronal c-fibers, which, in turn, trigger the release of histamine and other pro-inflammatory/immunosuppressive mediators from dermal mast cells. These events contribute to the development of various types of cutaneous pathologies, including the non-melanoma cancers, BCC and squamous cell carcinoma [2–5].

Because early disease is mostly responsive to standard treatments, implementation of expensive and often prolonged immunotherapies is usually considered unnecessary in the treatment of BCC, unlike that of advanced, invasive solid and hematological malignancies. This scenario

* Corresponding authors at: Department of Immunology, Faculty of Health Sciences, University of Pretoria, P O Box 667, Pretoria, 0001, South Africa.
*E-mail addresses:* mahlatse.kgokolo@up.ac.za (M.C.M. Kgokolo), bernardo.rapoport@up.ac.za (B.L. Rapoport).

https://doi.org/10.1016/j.tranon.2023.101867
Received 1 October 2023; Received in revised form 30 November 2023; Accepted 13 December 2023
Available online 2 February 2024

must, however, be viewed against the backdrop of BCC remaining the most frequently diagnosed cancer globally, together with a rising incidence among those aged 50 years and older [6,7]. Moreover, those who have experienced frequent occurrences (>6) are at increased risk for the development of malignancies at other anatomical sites [8,9]. Mechanistically, this association of BCC with development of other types of cancer has been linked to an increased prevalence of germline mutations in DNA repair genes. These underpin and are indicative of "frequent BCC development as an external marker of inherited cancer risk". A potential caveat, however, is that defective repair of damaged tumor DNA, particularly defective mismatch repair, results in augmentation of tumor immunogenicity due to an increased tumor mutational burden (TMB). This, in turn, potentiates the anti-tumor efficacy of co-inhibitory immune checkpoint (ICP)-targeted immunotherapy [10,11].

Immune checkpoints are of two major types, co-inhibitory and co-stimulatory, with the former representing the primary targets of monoclonal antibody (mAb)-based cancer immunotherapy. These are most commonly PD-1 (programmed cell death protein 1, CD274) and its ligand (PD-L1, CD279), as well as CTLA-4 (cytotoxic T-lymphocyte-associated protein 4, CD152), and, more recently LAG-3 (lymphocyte activation gene 3, CD223) and TIM-3 (T cell immunoglobulin and mucin domain 3, CD366). These co-inhibitory ICPs are expressed on various cell types in the tumor microenvironment (TME), including immune suppressor cells of the adaptive and innate immune systems, as well as tumor cells *per se* and cancer-associated fibroblasts, among others [12–14]. In addition, co-inhibitory soluble ICPs (sICPs) have also been detected in the systemic circulation of cancer patients with various types of advanced malignancies, including, but not limited to, melanoma and cancers of the breast, esophagus, head and neck, lung and stomach [15–20].

These cell-free soluble variants of co-inhibitory ICPs are likely to originate from the tumor *per se*, as well as from the heterogeneous resident and infiltrating cells that populate the TME. They are derived from proteolysis of the membrane-associated forms, or by formation of functional, secreted isoforms resulting from alternative splicing of precursor mRNA [21,22]. Importantly, these systemic co-inhibitory sICPs not only retain their immunosuppressive activities, but can also attenuate the therapeutic efficacy of ICP-targeted monoclonal antibodies [23].

We have previously reported that the plasma levels of five co-inhibitory sICPs, namely, CTLA-4, LAG-3, PD-1, PD-L1 and TIM3, are markedly elevated in BCC patients compared to those in the plasma of a group of healthy control participants [24]. However, measurements of co-stimulatory sICPs, or of dual-active checkpoints were not undertaken in this study [24]. Accordingly, the current study encompasses simultaneous measurement of an extended panel of all three categories of sICPs using stored plasma from the same cohort of BCC patients and a group of healthy control participants recruited to the original study [24]. In addition, we have measured the plasma levels of seven humoral immunosuppressive factors, which are positively linked to the activities of various types of immune suppressor cells, namely the enzymes, arginase 1 [25] and fibroblast activation protein (FAP) [26,27], the chemokine, Regulated upon Activation Normal T cell Expressed and Presumably Secreted (RANTES, CCL5) [28] and the cytokines, interleukin (IL)−10 [29] and transforming growth factor-β1 (TGF-β1) [30], as well as the M2-type macrophage markers, soluble CD163 (sCD163) [31] and sCD206 [32]. These were correlated with the levels of the various sICPs.

## Patients

Ethics approval was granted by the Research Ethics Committee of the Faculty of Health Sciences, University of Pretoria (Ethics Committee Approval Number: 356/2020). Advance written informed consent was obtained from all patients and control participants. The study population consisted of 40 South African patients (12F:28 M; mean age ±SD: 69.13 ± 11.20 years) with BCC attending the Dermatology Screening Clinic at Steve Biko Academic Hospital, Pretoria, South Africa. Patients aged 18 years and older, with a histologically confirmed diagnosis of BCC of varying subtypes were included. Those with known active acute or chronic infections were excluded. Patients with a diagnosis of other malignant tumors, which could potentially elevate the plasma levels of soluble ICPs, were also excluded. Patients were almost exclusively of Caucasian ethnicity ($n$ = 38; 11F:27 M), as well as one female and one male of African and Asian ethnicity, respectively. The various histological diagnoses [33] and anatomical sites of the malignancy are shown in Table 1. Of these, 27 patients had newly diagnosed disease, and 13 patients had recurrent disease (8 patients with second lesions, 4 patients with third lesions and 1 patient with a fourth lesion). As described by Pampena et al., "infiltrative BCC mostly appeared on the head and neck as an amelanotic hypopigmented plaque or papule, displaying ulceration on dermoscopic examination, along with arborizing and fine telangiectasia. Shiny white structures were also frequently observed. Multivariate analysis allowed us to define a clinical-dermoscopic profile of infiltrative BCC" [34]. The control group consisted of 20 participants (5F:15 M; mean age ±SD: 49.95 ± 14.59 years). The age difference between patients and control participants was significantly different ($p$ = 0.00001), underscoring the difficulty in recruiting healthy, older age-matched control subjects.

**Table 1**
Numbers of patients with: a) distinct clinical types of basal cell carcinoma (BCC); and b) basal cell carcinomas at distinct anatomical sites.

| a. Clinical subtype of BCC | b. Anatomical site |
|---|---|
| Adenoid ($n$ = 1)* | Cheek ($n$ = 3)*,+ |
| Basosquamous ($n$ = 3) | Chest ($n$ = 2) |
| Infiltrating ($n$ = 22) | Ear ($n$ = 4) |
| Infiltrating with squamous differentiation ($n$ = 4)# | Forearm ($n$ = 4) |
| Keratotic ($n$ = 1)## | Forehead ($n$ = 2) |
| Micronodular ($n$ = 2) | Lower limb ($n$ = 5) |
| Nodular ($n$ = 5) | Neck ($n$ = 2) |
| Pigmented, nodular ($n$ = 1)+,### | Nose ($n$ = 13)0 |
| Superficial ($n$ = 1)0 | Shoulder ($n$ = 1) |
| | Temple ($n$ = 2) |
| | Upper anterior chest ($n$ = 2) |

* Numbers of patients are shown in parenthesis;.
\+ African patient; 0Asian patient.
\# Infiltrating with squamous differentiation = the presence of histopathological features of BCC with squamous differentiation;.
\## Keratotic = BCC with focal areas of keratinization;.
\### The pigmented BCC was nodular.

Micrographs of representative samples from three of our BCC patients with different subtypes of disease (infiltrating BCC with squamous differentiation; micronodular BCC; and nodular BCC) are shown in Supplementary Figures 1, 2 and 3.

## Methods

Venous blood was collected in ethylenediaminetetraacetic acid (EDTA) vacutainers in the morning between 08H00 and 10H00 and processed within 30 min to separate the plasma component by centrifugation, which was then aliquoted and stored at minus 70 °C. Plasma was used as the matrix for analysis of the sICPs and the other seven biomarkers viz., arginase 1, FAP, RANTES, IL-10, TGF-β1, CD163 and CD206, resulting in a total of 24 different biomarkers, as opposed to the 5 biomarkers analyzed in our original study.

### *Measurement of the soluble immune checkpoint proteins*

A Human Immuno-Oncology Checkpoint Protein Panel (Milliplex® MAP Kit, Merck, KgaA, Darmstadt, Germany), which included an expanded range of sICPs relative to that which we had used previously in the setting of BCC was applied to simultaneously determine the plasma

concentrations of seven co-inhibitory sICPs, namely BTLA, CTLA-4, PD-1, PD-L1, PD-L2, LAG-3 and TIM-3; eight co-stimulatory sICPs, namely CD27, CD28, CD40, CD80, CD86, GITR, GITRL, and ICOS; and two dual-active sICPs, namely HVEM and TLR2. The methodology was followed as per the manufacturer's instructions and as described previously [24]. The levels of the 17 sICPs were assayed using a Bio-Plex Suspension Array platform (Bio-Rad Laboratories Inc., Hercules, CA, USA). The Bio-Plex Manager software 6.0 was used for bead acquisition and analysis of median fluorescence intensity. The results are reported as picograms (pg)/mL plasma. In addition to comparing plasma levels of the soluble co-inhibitory and co-stimulatory immune checkpoints between the entire cohorts of BCC patients and healthy controls, the following additional sub-group analyses were also performed: i) a comparison of the levels of the sICPs in BCC patients with newly diagnosed ($n = 27$) and recurrent disease ($n = 13$); recurrent disease was defined as malignancy that had returned at any site after a period of time during which the patient was in remission following treatment; ii) associations of age with plasma levels of the individual soluble immune biomarkers in the entire cohort of BCC patients using age cut-off values of $\leq$70 and >70 years ($n = 20$ in each sub-group with respective mean ages of 61±10 years and 77±3 years); and iii) measurement of the levels of the sICPs in BCC patients with aggressive disease (infiltrative, infiltrative with squamous differentiation, basosquamous and micronodular, $n = 31$) versus less aggressive disease (nodular, adenoid, keratotic, pigmented and superficial $n = 9$)

*Measurement of arginase 1*

A Human ARG1 ELISA Kit (E-EL-H0497, Elabscience, Houston, TX, USA) was employed for measuring the levels of arginase 1 present in the stored plasma samples. The methodology was followed as outlined by the manufacturer. Briefly, standards and samples (100 μL) were added to the appropriately designated wells of a 96-well plate. The plate was sealed and incubated at 37 °C for 1.5 h. Following the incubation period, the well contents were aspirated and 100 μL of biotinylated detection antibody was immediately added to each well and the plate incubated for an additional one hour at 37 °C. The plate was washed three times using an automated plate washer (BioTek Instruments Inc. Winooski, Vermont, USA). Horseradish peroxidase (HRP) conjugate working solution (100 μL) was added to each well, and the plate incubated at 37 °C for 30 min. The plate was then washed five times using an automated plate washer, followed by the addition of 90 μL of substrate reagent to each well, and the plate was incubated at 37 °C for an additional 15 min protected from light. The reaction was stopped by the addition of stop solution (50 μL) to each well and the optical density (OD) was measured immediately at 450 nm using a plate spectrophotometer (BioTek Instruments Inc.).

A standard curve, generated from the ODs obtained for the standards of known concentration, was used to determine the concentration of arginase 1 in the individual samples. Results are presented as nanograms (ng)/mL.

*Measurement of fibroblast activation protein*

Fibroblast activation protein levels were determined in the stored plasma samples using a Human Circulating Cancer Biomarker Kit (Milliplex® MAP Kit, Merck, KgaA, Darmstadt, Germany). The methodology was followed as described above for the immune checkpoint proteins. The results are reported as pg/mL

*Measurement of regulated upon activation normal T cell expressed and presumably secreted*

Levels of RANTES present in the stored plasma samples were determined using a Human RANTES ELISA Kit (E-EL-H6006, Elabscience, Houston, TX, USA). The samples were diluted 20-fold and the methodology was followed as outlined by the manufacturer and briefly described above for the measurement of arginase 1. Results are presented as ng/mL.

*Measurement of transforming growth factor-β1*

Prior to the analysis of the plasma samples for TGF-β1 concentrations, latent TGF-β1 was activated to the functional immuno-reactive form by the addition of 40 μL 1 N hydrochloric acid (HCl) to 280 μL of plasma diluted 8-fold. Following 10 min of incubation at room temperature, the samples were neutralized by the addition of 40 μL 1.2 M sodium hydroxide (NaOH)/ 0.5 M HEPES [4-(2-hydroatentxyethyl)−1-piperazineethanesulfonic acid]. Samples were then immediately assayed for TGF-β1 levels using a Human TGF- beta1 ELISA Kit (E-EL-0162, Elabscience, Houston, TX, USA). The same methodology was followed as described above for the arginase 1 ELISA. Results are presented as ng/mL.

*Measurement of interleukin-10*

Plasma levels of IL-10 were determined using a Human IL-10 ELISA Kit (E-EL-H6154, Elabscience, Houston, TX, USA). The samples were diluted 2-fold and the methodology was followed as outlined above for the measurement of arginase 1. Results are presented as pg/mL.

*Measurement of CD163*

A Human CD163 SimpleStep ELISA (ab274394, Abcam, Cambridge, UK) was used to determine the concentration of CD163 in the stored plasma samples. The methodology was followed as instructed by the manufacturer. The standards and diluted samples (50 μL) were added to the appropriate wells followed by the addition of 50 μL of antibody cocktail. The plate was sealed and incubated at room temperature for one h with gentle agitation (Thomas Scientific, Swedesboro, NJ, USA). Following the incubation period, the plate was washed three times using an automated plate washer (BioTek Instruments Inc.). A 100 μL volume of 3,3′,5,5′-tetramethylbenzidine (TMB) development solution was added to each well and the plate incubated, protected from light, for 10 min at room temperature. The reaction was stopped by the addition of 100 μL stop solution and the OD was measured immediately at 450 nm using a plate spectrophotometer (BioTek Instruments Inc.). The results are presented as pg/mL.

*Measurement of CD206*

Levels of CD206 were measured by means of a Human Mannose Receptor ELISA (ab277420, Abcam). Following dilution (20-fold), the samples and standards (100 μL) were added to the appropriate wells of the antibody-coated plate provided. The plate was sealed and incubated for 2.5 h at room temperature with gentle shaking (Thomas Scientific). The plate was washed four times using an automated wash station (BioTek Instruments Inc.) followed by the addition of 100 μL of biotinylated antibody. The plate was incubated for a further one hour as described above followed by an additional four washes. Prepared streptavidin solution (100 μL) was added to each well and the plate incubated for 45 min at room temperature with shaking whereafter the plate was washed a final four times. A 100 μL volume of TMB substrate reagent was added to each well and the plate incubated, protected from light, at room temperature for 30 min. The reaction was stopped by the addition of 50 μL stop solution and the OD was measured immediately at 450 nm using a plate spectrophotometer (BioTek Instruments Inc.). The results are presented as ng/mL.

**Expression and statistical analysis of results**

The primary hypothesis was that there was a significant difference in

**Table 2**
Comparison of the systemic concentrations of soluble co-stimulatory, co-inhibitory and dual immune checkpoint molecules in patients with basal cell carcinoma and control participants.

| Soluble immune checkpoints (pg/mL) | Patients with basal cell carcinoma ($n = 40$) | Control participants ($n = 20$) | $p\leq$ |
|---|---|---|---|
| CD27 | 3360 (2363 - 4970) | 1410 (1259 - 2172) | 0.0002 |
| CD28 | 17,047 (8487 - 30,677) | 11,314 (7236 - 14,883) | 0.2523 |
| CD40 | 1308 (968 - 1779) | 1222 (769 - 1349) | 0.4148 |
| ICOS | 15,359 (7591 - 20,308) | 12,902 (7980 - 15,316) | 0.3428 |
| GITR | 1217 (664 - 1795) | 698 (228 - 1222) | 0.0538 |
| GITRL | 2527 (1470 - 3599) | 2107 (1784 - 2724) | 0.3799 |
| CD86 | 2215 (793 - 3292) | 1636 (781 - 2144) | 0.2427 |
| CD80 | 1450 (863 - 2161) | 1212 (781 - 1590) | 0.3428 |
| PD-1 | 10,978 (5714 - 14,351) | 2524 (1832 - 3038) | 0.0000 |
| PD-L1 | 1740 (773 - 1980) | 228 (139 - 274) | 0.0000 |
| PD-L2 | 14,705 (13,102 - 16,375) | 12,008 (10,670 - 14,023) | 0.0011 |
| CTLA-4 | 744 (422 - 1129) | 126(56- 241) | 0.0000 |
| TIM-3 | 7519 (6619 - 8157) | 2328(1967 - 2667) | 0.0000 |
| LAG-3 | 388,288 (243,248 - 540,480) | 11,106 (6595 - 15,093) | 0.0000 |
| BTLA | 12,284 (8754 - 19,151) | 25,439 (17,274 – 32,427) | 0.0061 |
| TLR-2 | 17,696 (10,473 - 24,211) | 15,731 (12,262 - 19,913) | 0.6437 |
| HVEM | 2052 (1894 - 2317) | 1299 (1263 - 1458) | 0.0000 |

*Results are expressed as the median values with 95 % confidence intervals in parenthesis.

the plasma levels of the co-inhibitory sICPs and other systemic test biomarkers between BCC patients and healthy controls. Descriptive statistics were used to tabulate patient characteristics. The Shapiro-Wilk test was used to test for normality. All the variables tested were not normally distributed and therefore non-parametric statistics were used (see supplementary Table 1). Accordingly, non-parametric methods were used to compare levels of the various test biomarkers between BCC patients and healthy controls. A correlation matrix report was used to identify correlations between variables (or subsets of variables) within the subset, using Spearman *p*-values to define significance. A *p*-value of $<0.05$ was considered statistically significant. NCSS 2021 software for Windows (USA) was used for statistical analyses.

## Results

### *Soluble immune checkpoints*

These results are shown in Table 2. The plasma concentrations of 6 co-inhibitory sICPs (PD-1, PD-L1, PD-L2, CTLA-4, TIM-3, and LAG-3) and two co-stimulatory sICPs (CD27, and GITR) and one dual (HVEM) sICP were significantly elevated in the cohort of BCC patients relative to those of the group of control participants ($p \leq 0.0538$ -$p \leq 0.0000$). The fold increases in the median values were 15.9, 34.9, 4.3, 7.6, 3.2 and 1.2 for CTLA-4, LAG-3, PD-1, PD-L1, TIM-3 and PD-L2, respectively. The fold increases in the median values were 3.9 and 1.7, for CD27 and GITR respectively. The plasma concentrations of BTLA were significantly decreased in the cohort of BCC patients relative to those of the group of control participants ($p \leq 0.0061$), with a fold decrease in the median value of 2. Most notable were the differences in the median plasma levels of CTLA-4 in BCC patients (744 pg/mL compared to healthy controls 126 pg/mL; $p<0.0000$); those of LAG-3 (388,288 pg/mL compared to 11,106 pg/mL; $p<0.0000$); and those of TIM-3 (7519 pg/mL compared to 2328 pg/mL; $p<0.0000$).

**Table 3**
Comparison of the systemic concentrations of soluble co-stimulatory, co-inhibitory and dual immune checkpoint molecules in patients with newly diagnosed and recurrent basal cell carcinoma.

| Soluble immune checkpoints (pg/mL) | Patients with newly diagnosed BCC ($n = 27$) | Patients with recurrent BCC ($n = 13$) | $p\leq$ |
|---|---|---|---|
| CD27 | 4306 (3144 - 5051) | 3096 (1157 - 8215) | 0.6754 |
| CD28 | 20,005 (16,492 - 33,239) | 13,023 (10,431 - 28,652) | 0.7728 |
| CD40 | 358 (1160 −1721) | 1149 (922 −1785) | 0.8061 |
| COS | 17,225 (12,361 - 21,737) | 9564 (7258 - 19,701) | 0.4105 |
| GITR | 1303 (1155 - 2248) | 964 (562 - 1967) | 0.3122 |
| GITRL | 3034 (2240 - 3866) | 2480 (1439 - 3754) | 0.5159 |
| CD86 | 2610 (2008 - 4287) | 978 (864 - 3777) | 0.4356 |
| CD80 | 1674 (1294 - 2172) | 1209 (796 - 2279) | 0.5539 |
| PD-1 | 12,733 (9610 - 17,047) | 7721 (5164 - 16,156) | 0.4974 |
| PD-L1 | 1812 (1334 - 2308) | 832 (719 - 1989) | 0.4271 |
| PD-L2 | 14,795 (13,919 - 16,660) | 14,704 (13,013–17,174) | 0.7617 |
| CTLA-4 | 885 (722 - 1543) | 537 (420 - 1257) | 0.5734 |
| TIM-3 | 7855 (7063–9053) | 6974 (4824–9507) | 0.0912 |
| LAG-3 | 414,401 (328,221–524,201) | 342,947 (256,669–512,433) | 0.4703 |
| BTLA | 14,866 (11,737–22,199) | 9624 (6957–20,039) | 0.4441 |
| TLR-2 | 19,498 (15,524–26,115) | 11,036 (1463–3898) | 0.4974 |
| HVEM | 2028 (15,524–26,115) | 2112 (1463–3898) | 0.8511 |

*Results are expressed as the median values with 95 % confidence intervals in parenthesis.

**Table 4**
Comparison of the systemic concentrations of soluble co-stimulatory, co-inhibitory and dual-active immune checkpoint molecules in patients with basal cell carcinoma stratified according to age.

| Soluble immune checkpoints (pg/mL) | Patients with age ≤ 70 years ($n = 20$) | Patients with Age > 70 years ($n = 20$) | $p\leq$ |
|---|---|---|---|
| CD27 | 3544 (1900 - 4971) | 3325 (2082 - 5520) | 0.6588 |
| CD28 | 21,282 (7773 - 30,896) | 13,820 (6923 - 33,697) | 0.9031 |
| CD40 | 1237 (821 - 1737) | 1335 (923 - 1978) | 0.6980 |
| ICOS | 13,053 (4306 - 22,638) | 16,339 (7435 - 25,667) | 0.6017 |
| GITR | 1005 (357 - 2085) | 1295 (564 - 2214) | 0.5978 |
| GITRL | 2494 (962 - 4273) | 3010 (1338 - 4947) | 0.4291 |
| CD86 | 2007 (581 - 3928) | 2478 (856 - 4792) | 0.4651 |
| CD80 | 1383 (704 - 2515) | 1596 (864 - 2573) | 0.4989 |
| PD-1 | 10,611 (4673 - 18,676) | 12,011 (4850 - 20,983) | 0.5117 |
| PD-L1 | 1341 (684 - 2375) | 1830 (774 - 2634) | 0.4612 |
| PD-L2 | 14,548 (12,745 - 16,929) | 14,904 (13,030 - 16,875) | 0.6395 |
| CTLA-4 | 602 (231 - 1291) | 854 (295 - 1579) | 0.9246 |
| TIM-3 | 7690 (5988 - 8349) | 7445 (6416 - 8496) | 0.9680 |
| LAG-3 | 351,057 (195,176 - 549,470) | 425,233 (243,248 - 655,803) | 0.2184 |
| BTLA | 12,171 (6311 - 22,207) | 12,285 (7390 - 21,837) | 0.9676 |
| TLR-2 | 17,004 (7192 - 27,211) | 17,696 (9240 - 32,146) | 0.7584 |
| HVEM | 2048 (1755 - 2318) | 2105 (1832 - 2572) | 0.6017 |
| Arginase 1 | 27 (26 – 55) | 26 (26 – 30) | 0.0785 |
| FAP | 135 (117 - 161) | 90 (49 - 111) | 0.0012 |
| RANTES | 187 (116 - 234) | 96 (62 - 132) | 0.0128 |
| CD163 | 223,990 (194,810 - 302,356) | 215,175 (181,406 - 316,999) | 0.8709 |
| CD206 | 223 (191 - 272) | 232 (175 - 285) | 0.9246 |
| IL-10 | 0 (0 – 0) | 0 (0 – 0.1) | 0.6799 |
| TGF-β1 | 7543 (4549 - 12,017) | 6849 (3458 - 11,687) | 0.6456 |

*Results are expressed as the median values with 95 % confidence intervals in parenthesis.

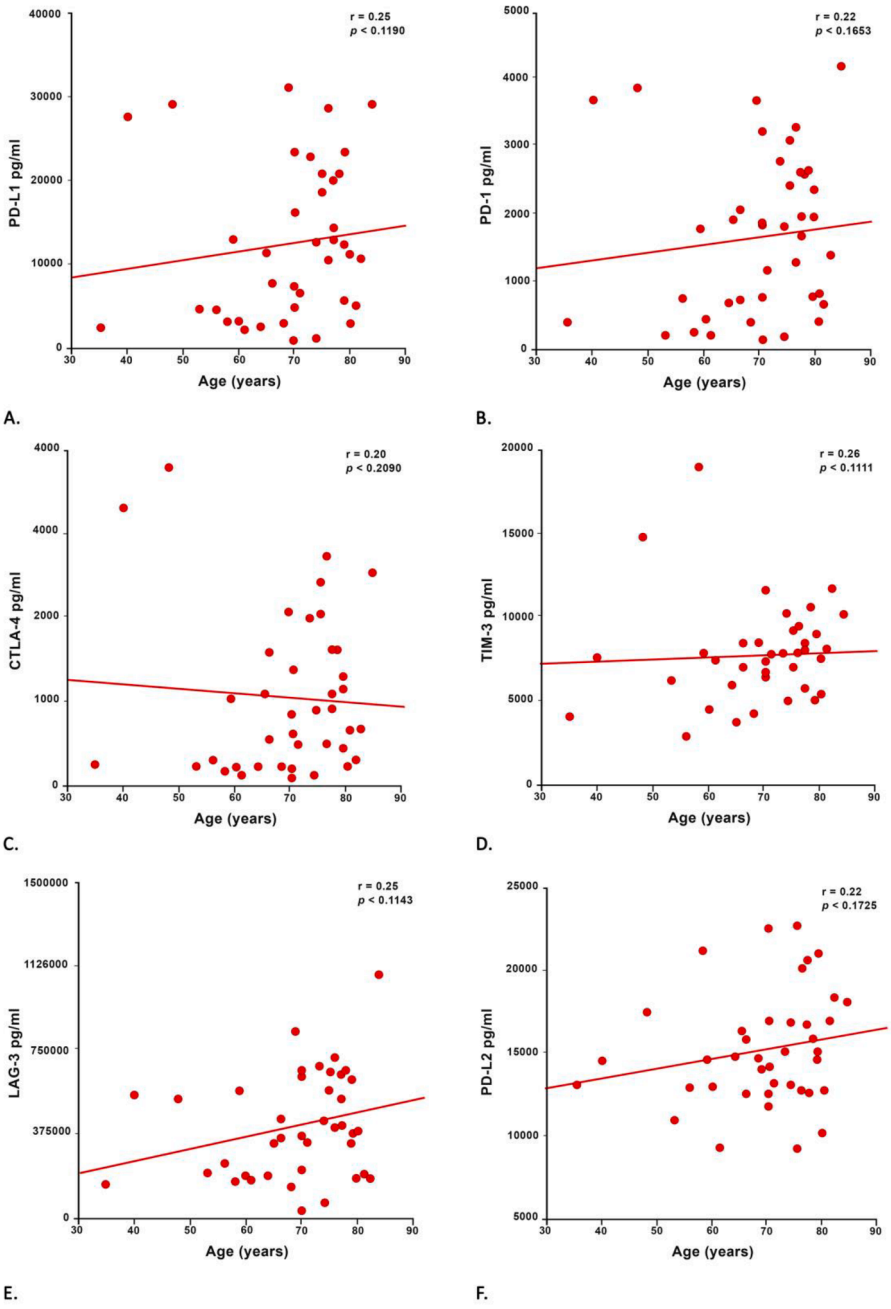


**Fig. 1.** Associations of the soluble co-inhibitory immune checkpoints, PD-1, PD-L1, CTLA-4, TIM-3, LAG-3, and PD-L2, with age.

*Comparison of soluble immune checkpoints between patients with newly diagnosed and recurrent basal cell carcinoma*

These results are shown in Table 3. There were no significant differences in the plasma concentrations of the 17 sICPs tested between patients with newly diagnosed and recurrent BCC.

*Effects of age on the plasma levels of the soluble immune checkpoints and other biomarkers*

Comparisons of the effects of age (≤70 and >70 years) on the plasma levels of the sICPs and other test biomarkers in patients with BCC are shown in Table 4. Except for RANTES, which decreased significantly with age, no significant age-related differences were found between the various sICPs and other biomarkers with respect to age. Similarly, as shown in Fig. 1, measurement of correlations of age with the plasma concentrations of six co-inhibitory sICPs (CTLA-4, PD-1, PD-L1, PD-L2, LAG-3 and TIM-3), revealed no statistically significant associations. These data exclude confounding effects of older age as a potential contributor to our findings of immune dysfunction in our cohort of BCC patients.

*Effects of disease aggression on the plasma levels of the soluble immune checkpoints and other biomarkers*

These results are shown in Table 5. Although no statistically significant differences were evident, patients with less aggressive disease showed a tendency towards higher levels of several of the sICPs and TGF-β1, possibly due to the smaller number of patients in this sub-group. Alternatively, albeit speculatively, this may reflect a more effective immune response in the setting of less aggressive disease.

**Table 5**
Comparison of the systemic concentrations of soluble co-stimulatory, co-inhibitory and dual-active immune checkpoint molecules in patients with aggressive and less aggressive basal cell carcinoma.

| Soluble immune checkpoints (pg/mL) | Patients with Aggressive types of BCC ($n = 31$) | Patients with Less aggressive types of BCC ($n = 9$) | $p \leq$ |
|---|---|---|---|
| CD27 | 3096 (1923 - 4932) | 5181 (2364 - 5520) | 0.3076 |
| CD28 | 13,023 (7773 - 24,361) | 31,684 (7907 - 49,048) | 0.0672 |
| CD40 | 1149 (821 - 1780) | 1313 1170 - 2677) | 0.2008 |
| ICOS | 12,865 (4738 - 18,595) | 20,309 (6256 - 34,575) | 0.1589 |
| GITR | 1080 (467 - 1796) | 1447 (564 - 3410) | 0.4466 |
| GITRL | 2480 (962 - 3359) | 4107 (1325 - 5492) | 0.1162 |
| CD86 | 1619 (581 - 3245) | 3564 (856 - 5960) | 0.0775 |
| CD80 | 1383 (731 - 2161) | 1757 (864 - 3036) | 0.1405 |
| PD-1 | 10,668 (4673 - 13,081) | 16,171 (5104 - 23,587) | 0.1789 |
| PD-L1 | 1408 (684 - 1967) | 2070 (759 - 3234) | 0.1589 |
| PD-L2 | 14,618 (13,030 - 16,759) | 15,102 (12,927 - 16,983) | 0.3731 |
| CTLA-4 | 667 (226 - 1072) | 1291 (295 - 1987) | 0.2779 |
| TIM-3 | 7820 (6130 - 8496) | 7411 (5078 - 8158) | 0.4862 |
| LAG-3 | 359,168 (195,176 - 531,667) | 549,470 (243,248 - 655,803) | 0.1089 |
| BTLA | 12,081 (7313 - 19,152) | 15,585 (8968 - 31,095) | 0.2007 |
| TLR-2 | 17,207 (8466 - 24,211) | 23,003 (10,473 - 41,316) | 0.1589 |
| HVEM | 2018 (1832 - 2438) | 2121 (1584 - 2942) | 0.7831 |
| Arginase 1 | 26 (26 – 32) | 26 (26 – 35) | 0.3501 |
| FAP | 115 (93 - 145) | 122 (4 - 179) | 0.9354 |
| RANTES | 132 (91 - 207) | 131 (61 - 234) | 0.9483 |
| CD163 | 238,292 (194,810 - 316,999) | 204,962 (137,052 - 235,419) | 0.0744 |
| CD206 | 220 (191 - 272) | 240 (51 - 285) | 0.8586 |
| IL-10 | 0 (0 – 0) | 0 (0 – 0.64) | 0.7575 |
| TGF-β1 | 5731 (4142 - 11,687) | 9012 (3536 - 12,925) | 0.6156 |

*Results are expressed as the median values with 95 % confidence intervals in parenthesis.

**Table 6**
Comparison of the systemic concentrations of arginase 1, RANTES, TGF-β1, FAP, IL-10, CD206, and CD163 in patients with basal cell carcinoma and control participants.

| Biomarker | Patients with basal cell carcinoma ($n = 40$) | Control participants ($n = 20$) | $p \leq$ |
|---|---|---|---|
| Arginase | 25 (25 - 29) | 25 (25 - 72) | 0.2897 |
| RANTES | 131 (97 – 175) | 91 (71 - 149) | 0.2097 |
| TGF-β1 | 7543 (4549 - 10,795) | 5829 (4184 - 6834) | 0.1469 |
| IL-10 | 0 (0 - 0) | 0 (0 – 4) | 0.1322 |
| FAP | 116 (94 - 130) | 109 (71 - 127) | 0.2425 |
| CD206 | 227 (192 - 251) | 188 (143–278) | 0.502 |
| CD163 | 218,017 (194,810 - 298,215) | 216,818 (133,047 - 272,483) | 0.2266 |

Results are expressed as median values with 95 % confidence limits in parenthesis.
Results for arginase 1, RANTES and CD206 are presented as ng/mL while those for TGF-β1, FAP, IL-10 and CD163 are presented as pg/mL.

*Arginase 1, RANTES, TGF-β1, FAP, IL-10, CD206, and CD163*

The comparison of the systemic concentrations of arginase 1, RANTES, FAP, TGF-β1, IL-10, CD206, and CD163 in patients with BCC and control participants are shown in Table 6. The plasma concentrations of RANTES (131 ng/mL compared to 91 ng/mL, $p \leq 0.2097$) and TGF-β1 (7.5 ng/mL compared to 5.8 ng/mL; $p \leq 0.1469$) were numerically increased in the cohort of BCC patients relative to those of the group of control participants. The plasma concentrations of arginase 1, FAP, IL-10, CD163, and CD206 were not significantly different in the cohort of BCC patients from those of the group of the control participants ($p \leq 0.2897$, 0.2425, 0.1322, 0.2266, and 0.5020, respectively).

*Correlations between TGF-β1 and the other biomarkers with the soluble immune checkpoint molecules*

As shown in the heat map in Fig. 2 and in Figs. 3–5, moderate-to-strong positive correlations were detected between TGF-β1, and eleven of the sICPs (LAG-3, $r = 0.8083$; PD1, $r = 0.7409$; PDL-1, $r = 0.7559$, CTLA-4, $r = 0.6740$; CD80, $r = 0.7674$; CD86, $r = 0.7580$; ICOS, $r = 0.6885$, CD28, $r = 0.6184$, GITR, $r = 0.7649$ and; GITRL $r = 0.7681$; TLR-2, $r = 0.6963$; all $p$ values were $<0.0000$).

No correlations between the sICPs and arginase 1, RANTES, FAP, IL10, CD163, and CD206 were detected in the cohort of BCC patients.

## Discussion

The current study, in which the plasma concentrations of 24 different soluble immune biomarkers were measured in patients with BCC, represents one of the most comprehensive with respect to immune checkpoint-mediated immune dysfunction in this condition. We confirmed our earlier findings that BCC is associated with significantly increased plasma levels of the co-inhibitory sICPs, sCTLA-4, sLAG-3, sPD-1, sPD-L1 and sTIM-3 [24] and extended these to include sPD-L2 and sBTLA, the levels of which were significantly elevated and decreased, respectively. As an additional extension of our earlier study, we also measured the plasma concentrations of the co-stimulatory sICPs, CD27, CD28, CD40, CD80, CD86, GITR, GITRL, and ICOS, as well as those of the dual-active sICPs, sHVEM (herpes virus entry mediator, CD270) and sTLR2 (Toll-like receptor 2, CD282). With respect to the co-stimulatory sICPs, the plasma levels of the majority of these were similar to those of the control subjects, with the exceptions of CD27 and GITR, the concentrations of which were significantly elevated, as was the level of the dual-active sICP, HVEM. Although speculative, the lower concentrations of sBTLA in the BCC group may relate to its interactions with HVEM, possibly complicating detection [35].

In addition to the seventeen soluble immune checkpoints, we also measured the plasma levels of seven humoral immune factors linked to the activation of various types of pro-tumorigenic immune suppressor cells. These are the enzymes arginase 1 (PMN-MDSC), FAP, RANTES/CCL5, sCD163 and sCD206 (all four linked to M2-type macrophages), as well as IL-10 and TGF-β1 (both linked to Tregs) [27–33,36]. Although the median plasma concentrations of all seven of these biomarkers did not differ significantly from those of the control group, a correlation heat map revealed selective, mostly strong correlations, of TGF-β1 with four of the co-inhibitory sICPs, namely (in order of the strength of the correlations), sLAG-3 >sPD-L1 >sPD-1 >sCTLA-4. These associations are particularly noteworthy since all four of these biomarkers are constitutively expressed by, and are prominent mediators of the immunosuppressive functions, of Tregs; TGF-β1 maintains Foxp3 expression and the immune regulatory functions of Tregs [36–42].

Given that the plasma levels of 6/8 of the co-stimulatory sICPs were comparable in the BCC and control groups, the increased levels of sCD27 and sGITR in the BCC cohort seemed counterintuitive. However, as shown previously, CD27, which mediates its co-stimulatory effects on T cells, B cells, and natural killer (NK) cells via interactions with CD70, is also expressed on murine Tregs, driving Treg-mediated suppression of anti-tumor immunity [43]. If evident in humans, this activity of CD27 may explain the unexpected increase in the systemic levels of sCD27 in the cohort of BCC patients [43]. However, no correlation of CD27 with TGF-β1 was evident in the current study. In the case of GITR, this co-stimulatory ICP is highly expressed on human solid tumors, particularly non-small cell lung carcinoma, renal cell carcinoma, and melanoma, which are associated with increased numbers of GITR-expressing $CD4^+Foxp3^+$ Tregs in the TME [44]. In this context, $CD4^+$ $Foxp3^+$ Tregs, which co-express high levels of GITR and CTLA-4, have been reported to

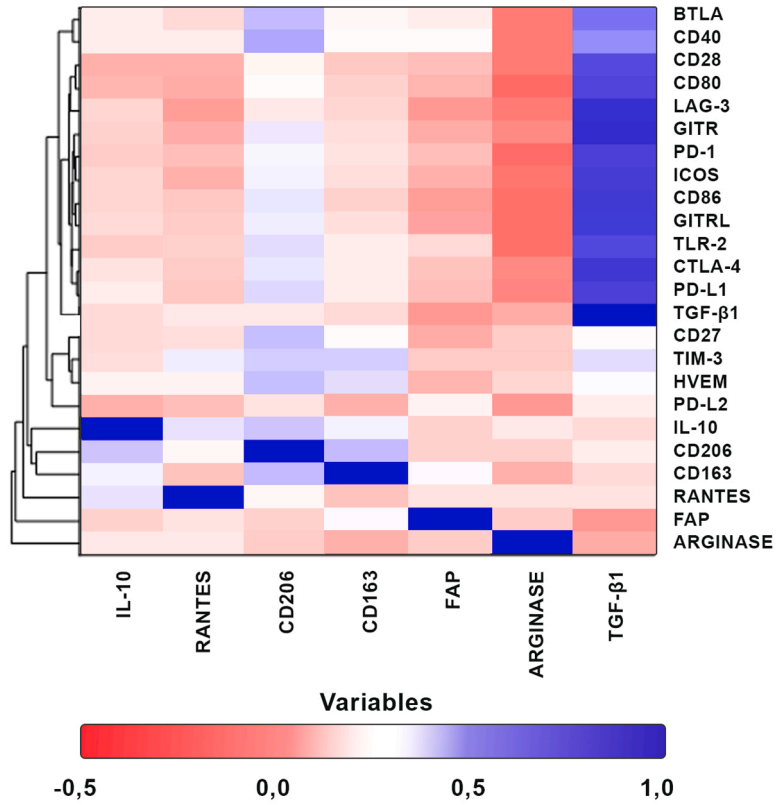


**Fig. 2.** Correlations between IL-10, RANTES, CD206 CD163, FAP, Arginase 1, and TGF-β1 with the soluble immune checkpoint molecules.

suppress anti-tumor immunity in humans with either primary hepatocellular carcinoma or liver metastases from colorectal cancer [45]. Unlike CD27, the associations of GITR and GITRL with TGF-β1 were strong.

Although TGF-β1 is produced by many different cell types, only Tregs, as well as B cells, megakaryocytes and platelets, possess the cellular machinery to produce and convert latent, inactive TGF-β1 to its biologically active, immunosuppressive form [46,47]. The mechanisms utilized by Tregs do, however, differ somewhat from those used by the other cell types. They involve binding of the latency-associated peptide of the cytokine to the trans-membrane protein, glycoprotein-A repetition predominant (GARP) protein, via disulfide linkage, enabling interaction of this complex with membrane αVβ6 and αVβ8 integrins, resulting in the presentation and release of active TGF-β1. These are key events in the pro-tumorigenic activity of the Treg/TGF-β1 axis in the TME and are achieved via suppression of the anti-tumor reactivity of cells of both the adaptive and innate immune systems, as well as by interactions with structural cells [47–49]. In the case of structural cells, TGF-β1 has been reported to induce cancer-associated fibroblasts to promote fibrosis and immunosuppression via expression and release sPD-L1 packaged in extracellular vesicles [50,51].

Notwithstanding those observed with sGITR and sGITRL, somewhat surprisingly, strong heat map correlations of four other co-stimulatory sICPs with TGF-β1 were also evident in the current study, the order of strength of the correlations being sCD80> sCD86> sICOS> sCD28. Although these findings are somewhat more difficult to explain, they may represent a compensatory mechanism to counteract the immunosuppressive activity of the Treg/TGF-β1 axis.

Clinically, BCC is the most common cancer in the USA, with more than 2 million cases diagnosed annually [52]. Localized disease is typically cured with minimally invasive treatment modalities, including surgery and topical or photodynamic therapy, and is associated with good long-term outcomes [53]. However, some BCC patients may develop recurrent, local invasion, or metastatic disease, resulting in substantial morbidity or mortality [54]. Management of these BCC patients may be clinically challenging. There are no standard treatment guidelines for locally advanced or metastatic BCC. Current treatments include surgery, local treatment with topical creams, radiation therapy, and targeted therapies with hedgehog inhibitors, and immune checkpoint inhibitors [55]. In this latter context, Lipson et al. have confirmed that the majority of BCC patients express elevated levels of PD-L1 in TME and/or tumor cells. These researchers who analyzed 40 biopsies from BCC patients, demonstrated expression of PD-L1 on tumor cells in 9/40 (22 %) cases. PD-L1 was also detected on tumor-infiltrating lymphocytes (TILs) and associated macrophages in biopsies of 33/40 (82 %) BCC patients [56].

The findings of the aforementioned study resulted in the evaluation of the PD-1 antagonist, cemiplimab-rwlc, in BCC patients with advanced, or refractory disease. This phase 2 study demonstrated favorable activity in patients with metastatic or locally advanced BCC with progressive disease, or those who were intolerant of prior hedgehog inhibitor treatment in the second line setting. No predictive biomarker for response to cemiplimab-rwlc treatment was reported [57]. Based on the results of this phase 2 study, in February 2021, the USA Food and Drug Administration approved cemiplimab-rwlc for the management of the categories of BCC patients included in the above study [58]. Subsequently, cemiplimab-rwlc was also approved in Europe in June 2021 for the same indication (Libtayo®) [59]. Experts currently propose cemiplimab-rwlc as a first-line systemic alternative [60].

The present study documented high plasma levels of CTLA-4, LAG-3, PD-L1, PD-L2 and TIM-3, in the cohort of BCC patients, which correlated positively with TGF-β1. Concerning LAG-3 and TIM-3, the former is expressed by T cells, including Tregs, as well as by B cells, natural killer (NK) cells, and plasmacytoid DCs [61]. LAG-3 interacts with several ligands, including MHC class II and galectin-3, via interactions with MHC II expressed by T cells and tumor-infiltrating, LAG-3-expressing tolerogenic plasmacytoid DCs. These cells inhibit T cell proliferation and promote differentiation towards a Treg phenotype. Tregs which express LAG-3 interact with non-tolerogenic MHC class II+ DCs, resulting in

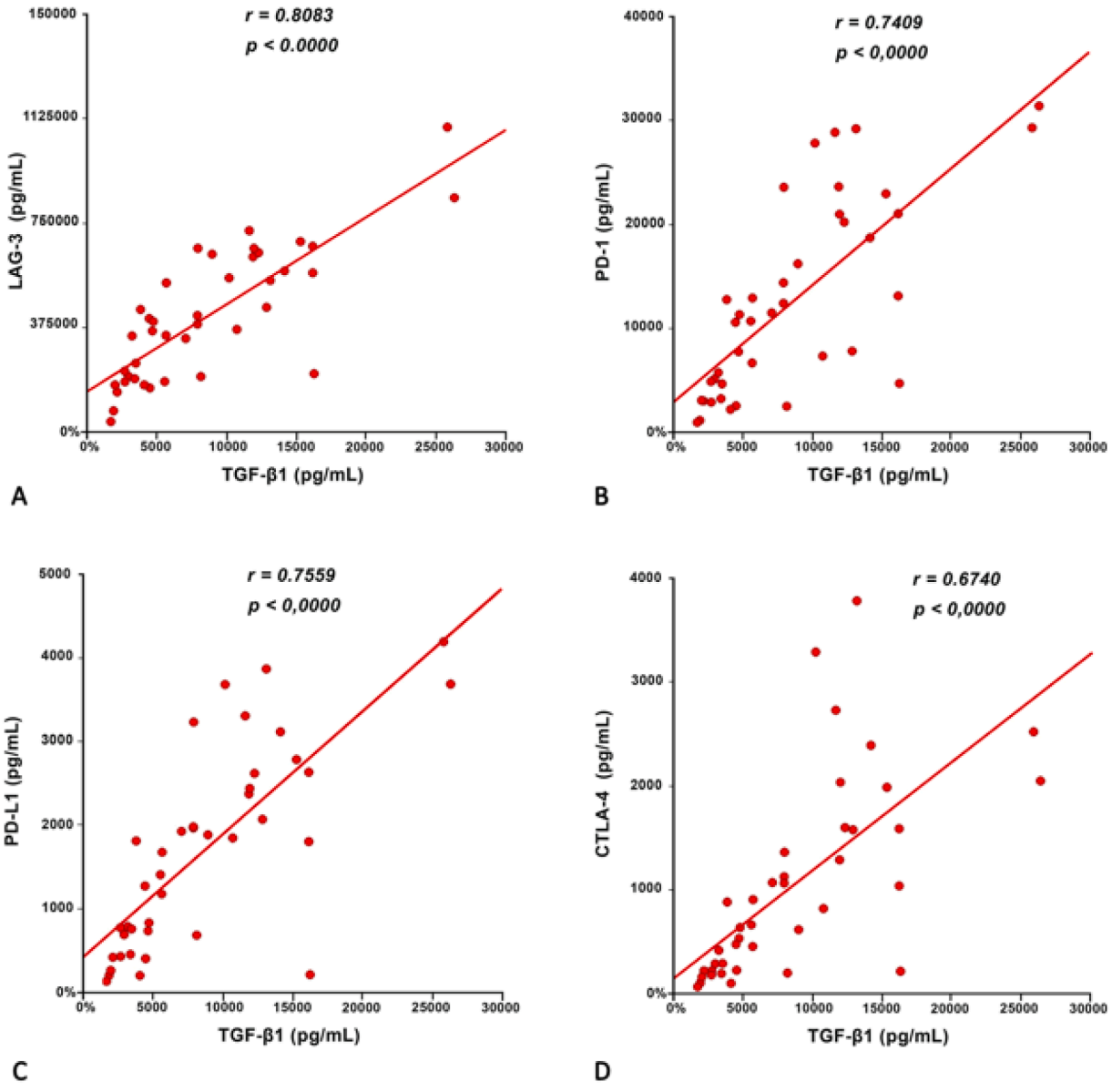


**Fig. 3.** Associations of the soluble co-inhibitory immune checkpoints, LAG-3, PD-1 and PD-L1, CTLA-4 with TGF-β1.

attenuation of both, the development and protective anti-tumor properties of these cells [61]. TIM-3, on the other hand is present in activated CD4+ and CD8+ T cells and interacts with various ligands, such as galectin-9, present on tumor cells and Tregs [62].

TGF-β1 is a multifunctional cytokine that acts as a tumor promoter or suppressor in a cell- and context-dependent manner. As a tumor promoter, the TGF-β1 pathway enhances cell proliferation, migratory invasion, and metastatic spread within the TME and suppresses immunosurveillance. TGF-β1 signaling contributes both to drug resistance and tumor escape and is also associated with poor clinical response to treatment. Several small molecules, such as TGF-β receptor kinase inhibitors, have been created to interact with the ATP-binding domain of the enzyme, inhibiting enzyme activity, and blocking the downstream signaling cascade [63]. Vactosertib (EW-7197) is a small molecule, orally available inhibitor of the kinase activity of TGF-β RI/ALK-5 [64]. Galunisertib (LY21557299) is a TGF-βRI kinase antagonist, which demonstrated activity by reducing lung and breast cancer cell growth and was safe in patients with various solid tumors in phase I studies [65]. TGF-β1-directed antibodies, which block ligand activation or prevent ligand-receptor binding activity are also under development. Fresolimumab (GC1008) is a human monoclonal antibody (mAb) that neutralizes TGF-β1 and TGF-β2. This agent was investigated in a phase 1 trial in 28 patients with malignant melanoma and one with renal cell carcinoma (RCC). Encouraging activity was shown in seven patients with partial responses.

Bintrafusp alfa (GSK-4045154, M7824, MSB0011359C) is an innovative first-in-class bifunctional fusion protein composed of a monoclonal antibody against PD-L1 fused to the extracellular domain of the TGF-βRII [66]. A multi-center, global single-arm phase II study (NCT04246489) will be conducted to assess the clinical activity and safety profile of Bintrafusp alfa in platinum-exposed cervical cancer [67].

Limitations of the study include: i) this was a single center study with potential selection bias; ii) no post-treatment follow-up; iii) lack of correlation with the same biomarkers in the TME; iv) the sample size was adequate for comparison of the BCC cohort and controls; however, to compare the various sICPs in the different BCC subsets a larger patient cohort would be required to be adequately powered; v) validation of our findings might require a larger number of patients in a multi-center setting. We intend addressing these issues in future studies.,with a

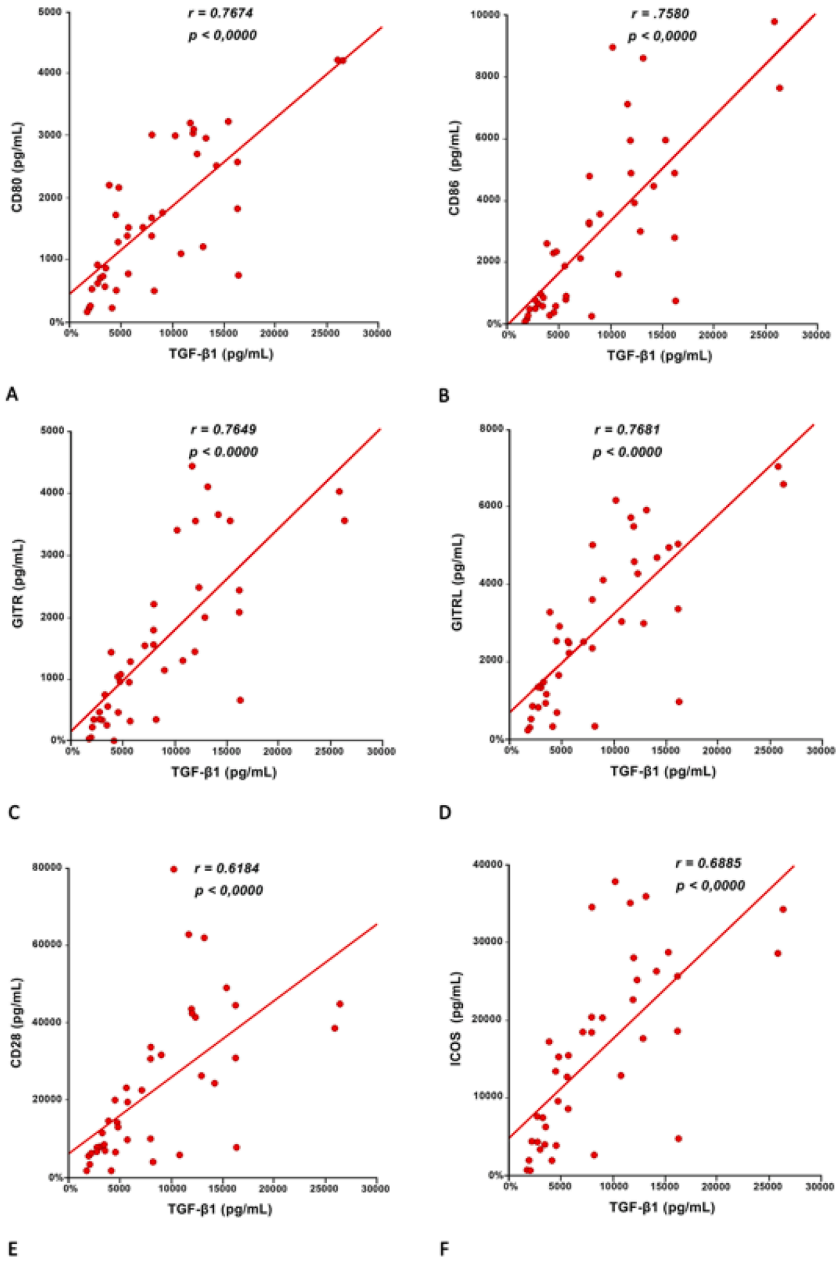


**Fig. 4.** Associations of the soluble co-stimulatory immune checkpoints, CD80, CD86, GITR, GITRL, CD28, and ICOS, with TGF-β1.

particular focus on the TME.

In closing, the current study has indicated the likely involvement of the TGF-β1/co-inhibitory ICP axis as being a driver of pro-tumorigenic, pro-invasive immunosuppression in advanced BCC. As a progression of our current research, our future BCC research program will focus on correlating the presence of Tregs in the circulation and TME with the systemic levels of sICPs and TGF-β1. The rationale underpinning this strategy is based on the findings of the current study and supported by published data, which have described the predominance of Tregs in both the TME and peritumoral skin of these patients [68–70]. Importantly, our study also provides a rationale for investigating the role of anti-PD-1-targeted mAbs in combination with other mAbs that target other co-inhibitory ICPs, such as CTLA-4 or LAG-3, or TIM-3, as well as in combination with anti-TGF-β1 strategies as recently proposed by van den Bulk et al. [71]. These agents may enable effective co-blockade. To our knowledge, anti-TGF-β agents have not been investigated in patients with advanced or metastatic BCC. Identification of predictive biomarkers of response in this clinical setting represents a crucial, unmet medical need.

## Conclusion

High plasma levels of co-inhibitory sICPs, and a positive correlation with TGF-β1, were detected in BCC patients. These features are suggestive of prominent pro-tumorigenic immunosuppressive activity. Inhibitory sICPs and plasma levels of TGF-β1 should therefore be investigated as possible predictors of response to treatment, as well as prognostic biomarkers in these patients. The current study provides a rationale for conducting clinical trials combining anti-PD-1 mAbs with anti-CTLA-4, anti-LAG-3 and anti-TIM-3 mAbs, or with anti-TGF-β1 mAbs in advanced BCC patients. Our findings also support investigating the use of these antibodies earlier in the course of this disease.

## Data availability

Data are available upon reasonable request. The data generated in

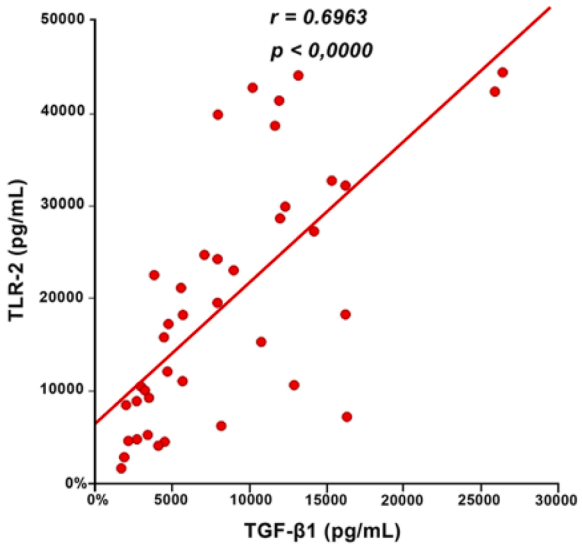


**Fig. 5.** Association of the dual-active soluble immune checkpoint, TLR-2, with TGF-β1.

this study are available on request from the corresponding author.

## Ethics statements

Patient consent for publication.
Not applicable.

## Ethics approval

This study was performed in accordance with the principles of the Declaration of Helsinki. The collection of specimens and associated clinical data used in this study was approved by the Research Ethics Committee of the Faculty of Health Sciences, University of Pretoria (Ethics Committee Approval Number: 356/2020).

## CRediT authorship contribution statement

**Mahlatse C.M. Kgokolo:** Conceptualization, Data curation, Writing – review & editing. **Nonkululeko Z. Malinga:** Conceptualization, Data curation, Investigation, Methodology, Project administration, Validation, Visualization, Writing – original draft, Writing – review & editing. **Helen C. Steel:** Conceptualization, Data curation, Formal analysis, Methodology, Resources, Validation. **Pieter W.A. Meyer:** Data curation, Formal analysis, Software. **Teresa Smit:** Data curation, Formal analysis, Software, Validation, Writing – review & editing. **Ronald Anderson:** Conceptualization, Data curation, Formal analysis, Investigation, Methodology, Project administration, Resources, Supervision, Validation, Visualization, Writing – original draft, Writing – review & editing. **Bernardo L. Rapoport:** Conceptualization, Data curation, Formal analysis, Funding acquisition, Methodology, Software, Writing – original draft, Writing – review & editing, Investigation, Resources, Supervision, Validation, Visualization.

## Declaration of competing interest

None of the authors has a conflict of interest to declare.

## Acknowledgments

The authors gratefully acknowledge the expert contributions of Ms Hannatjie van Wyk (administrative) and Ms Michell Greef (graphics, "Bits and Bytes") to preparation of the manuscript. We are grateful to the patients, their families, and referring physicians who made this study possible.

## Supplementary materials

Supplementary material associated with this article can be found, in the online version, at doi:10.1016/j.tranon.2023.101867.

## References

[1] D.I. Schlessinger, K.A. Reynolds, M.A. Dirr, S.A. Ibrahim, A.F. Yanes, J.M. Lazaroff, V. Godinez-Puig, B.R. Chen, A.O. Kurta, J.K. Cotseones, S.G. Chiren, K.C. Furlan, S. Iyengar, R. Behshad, D.M. DeHoratius, P. Denes, A.M. Drucker, L.M. Dzubow, J. R. Etzkorn, C.A. Harwood, J.Y.S. Kim, N. Lawrence, E.H. Lee, G.S. Lissner, A. A. Marghoob, R.N. Matin, A.R. Mattox, B.B. Mittal, J.R. Thomas, X.A. Zhou, D. Zloty, J. Schmitt, J.J. Kirkham, A.W. Armstrong, N. Basset-Seguin, E. M. Billingsley, J.S. Bordeaux, J. Brewer, M. Brown, M. Brown, S.A.B. Collins, M. C. Fargnoli, S.J. De Azevedo, R. Dummer, A. Eggermont, G.D. Goldman, M. Haedersdal, E.K. Hale, A. Hanlon, K.L. Harms, C.C. Huang, E.A. Hurst, G.K. In, N. Kelleners-Smeets, M. Kheterpal, B. Leshin, M. Mcdonald, S.J. Miller, A. Miller, E. N. Mostow, M. Trakatelli, K.S. Nehal, D. Ratner, H. Rogers, K.Y. Sarin, S.L. Soon, T. Stasko, P.A. Storrs, L. Tagliaferri, A.T. Vidimos, S.L. Wong, S.S. Yu, I. Zalaudek, N.C. Zeitouni, J.A. Zitelli, E. Poon, J.F. Sobanko, T.V. Cartee, I.A. Maher, M. Alam, Development of a core outcome set for basal cell carcinoma, J. Am. Acad. Dermatol. 87 (2022) 573–581, https://doi.org/10.1016/j.jaad.2022.04.059. PMID: 35551965.

[2] S. Ch'ng, R.A. Wallis, L. Yuan, P.F. Davis, S.T. Tan, Mast cells and cutaneous malignancies, Mod. Pathol. 19 (2006) 149–159, https://doi.org/10.1038/modpathol.3800474. PMID: 16258517.

[3] M. Lupu, A. Caruntu, C. Caruntu, L.M.L. Papagheorghe, M.A. Ilie, V. Voiculescu, D. Boda, C. Constantin, C. Tanase, M. Sifaki, N. Drakoulis, C. Mamoulakis, G. Tzanakakis, M. Neagu, D.A. Spandidos, B.N. Izotov, A.M. Tsatsakis, Neuroendocrine factors: the missing link in nonmelanoma skin cancer (Review), Oncol. Rep. 38 (2017) 1327–1340, https://doi.org/10.3892/or.2017.5817. PMID: 28713981; PMCID: PMC5549028.

[4] A.T. Slominski, M.A. Zmijewski, P.M. Plonka, J.P. Szaflarski, R. Paus, How UV light touches the brain and endocrine system through skin, and why, Endocrinology 159 (2018) 1992–2007, https://doi.org/10.1210/en.2017-03230. PMID: 29546369; PMCID: PMC5905393.

[5] A.T. Slominski, R.M. Slominski, C. Raman, J.Y. Chen, M. Athar, C. Elmets, Neuroendocrine signaling in the skin with a special focus on the epidermal neuropeptides, Am. J. Physiol. Cell Physiol. 323 (2022) C1757–C1776, https://doi.org/10.1152/ajpcell.00147.2022. PMID: 36317800; PMCID: PMC9744652.

[6] S. Wu, J. Han, W.Q. Li, T. Li, A.A Qureshi, Basal-cell carcinoma incidence and associated risk factors in U.S. women and men, Am. J. Epidemiol. 178 (2013) 890–897, https://doi.org/10.1093/aje/kwt073. PMID: 23828250; PMCID: PMC3775544.

[7] K. Schreuder, L. Hollestein, T.E.C. Nijsten, M. Wakkee, M.W.J. Louwman, A nationwide study of the incidence and trends of first and multiple basal cell carcinomas in the Netherlands and prediction of future incidence, Br. J. Dermatol. 186 (2022) 476–484, https://doi.org/10.1111/bjd.20871. PMID: 34726263.

[8] M.R. Karagas, E.R. Greenberg, L.A. Mott, J.A. Baron, V.L. Ernster, Occurrence of other cancers among patients with prior basal cell and squamous cell skin cancer, Cancer Epidemiol. Biomarkers Prev. 7 (1998) 157–161. PMID: 9488591.

[9] H.G. Cho, K.Y. Kuo, S. Li, I. Bailey, S. Aasi, A.L.S. Chang, A.E. Oro, J.Y. Tang, K. Y. Sarin, Frequent basal cell cancer development is a clinical marker for inherited cancer susceptibility, JCI Insight 3 (2018) e122744, https://doi.org/10.1172/jci.insight.122744. PMID: 30089731; PMCID: PMC6129130.

[10] K.M. Bever, D.T. Le, DNA repair defects and implications for immunotherapy, J. Clin. Invest. 128 (2018) 4236–4242, https://doi.org/10.1172/JCI122010. PMID: 30272580; PMCID: PMC6159999.

[11] J. Zhang, D.J.H. Shih, S.Y Lin, Role of DNA repair defects in predicting immunotherapy response, Biomark. Res. 8 (2020) 23, https://doi.org/10.1186/s40364-020-00202-7. PMID: 32612833; PMCID: PMC7325270.

[12] S.C. Wei, C.R. Duffy, J.P. Allison, Fundamental mechanisms of immune checkpoint blockade therapy, Cancer Discov 8 (2018) 1069–1086, https://doi.org/10.1158/2159-8290.CD-18-0367. PMID: 30115704.

[13] H. Zhang, P. Dutta, J. Liu, N. Sabri, Y. Song, W.X. Li, J. Li, Tumour cell-intrinsic CTLA4 regulates PD-L1 expression in non-small cell lung cancer, J. Cell Mol. Med. 23 (2019) 535, https://doi.org/10.1111/jcmm.13956. -342PMID: 30378264; PMCID: PMC6307812.

[14] K. Yoshikawa, M. Ishida, H. Yanai, K. Tsuta, M. Sekimoto, T. Sugie, Prognostic significance of PD-L1-positive cancer-associated fibroblasts in patients with triple-negative breast cancer, BMC Cancer 21 (2021) 239, https://doi.org/10.1186/s12885-021-07970-x. PMID: 33676425; PMCID: PMC7937297.

[15] D. Machiraju, M. Wiecken, N. Lang, I. Hülsmeyer, J. Roth, T.E. Schank, R. Eurich, N. Halama, A. Enk, J.C. Hassel, Soluble immune checkpoints and T-cell subsets in blood as biomarkers for resistance to immunotherapy in melanoma patients, Oncoimmunology 10 (2021) 1926762, https://doi.org/10.1080/2162402X.2021.1926762. PMID: 34104542; PMCID: PMC8158029.

[16] B. Han, L. Dong, J. Zhou, Y. Yang, J. Guo, Q. Xuan, K. Gao, Z. Xu, W. Lei, J. Wang, Q. Zhang, The clinical implication of soluble PD-L1 (sPD-L1) in patients with breast cancer and its biological function in regulating the function of T lymphocyte,

Cancer Immunol. Immunother. 70 (2021) 2893–2909, https://doi.org/10.1007/s00262-021-02898-4. PMID: 33688997; PMCID: PMC8423647.
[17] J. Yoshida, T. Ishikawa, T. Doi, T. Ota, T. Yasuda, T. Okayama, N. Sakamoto, K. Inoue, O. Dohi, N. Yoshida, K. Kamada, K. Uchiyama, T. Takagi, H. Konishi, Y. Naito, Y. Itoh, Clinical significance of soluble forms of immune checkpoint molecules in advanced esophageal cancer, Med. Oncol. 36 (2019) 60, https://doi.org/10.1007/s12032-019-1285-x. PMID: 31134385.
[18] N.E. Kushlinskii, E.S. Gershtein, V.L. Chang, E.A. Korotkova, A.A. Alferov, M. M. Kontorshchikov, N.Y. Sokolov, E.I. Karamysheva, N.A. Ognerubov, I.S. Stilidi, Prognostic significance of soluble forms of immune checkpoint PD-1/PDL1 receptor and ligand in blood plasma of gastric cancer patients, Klin. Lab. Diagn. 66 (2021) 139–146, https://doi.org/10.51620/0869-2084-2021-66-3-139-146. PMID: 33793112.
[19] A. Botticelli, I.G. Zizzari, S. Scagnoli, G. Pomati, L. Strigari, A. Cirillo, B. Cerbelli, A. Di Filippo, C. Napoletano, F. Scirocchi, A. Rughetti, M. Nuti, S. Mezi, P. Marchetti, The role of soluble LAG3 and soluble immune checkpoints profile in advanced head and neck cancer: a Pilot Study, J. Pers. Med. 11 (2021) 651, https://doi.org/10.3390/jpm11070651. PMID: 34357118; PMCID: PMC8304359.
[20] Y. Peng, C. Zhang, Z. Rui, W. Tang, Y. Xu, X. Tao, Q. Zhao, X. Tong, A comprehensive profiling of soluble immune checkpoints from the sera of patients with non-small cell lung cancer, J. Clin. Lab. Anal. 36 (2022) e24224, https://doi.org/10.1002/jcla.24224. PMID: 35019173; PMCID: PMC8841185.
[21] D. Gu, X. Ao, Y. Yang, Z. Chen, X. Xu, Soluble immune checkpoints in cancer: production, function and biological significance, J. Immunother. Cancer 6 (2018) 132, https://doi.org/10.1186/s40425-018-0449-0. PMID: 30482248; PMCID: PMC6260693.
[22] X. Zhu, J. Lang, Soluble PD-1 and PD-L1: predictive and prognostic significance in cancer, Oncotarget 8 (2017) 97671–97682, https://doi.org/10.18632/oncotarget.18311. PMID: 29228642; PMCID: PMC5722594.
[23] R. Sagawa, S. Sakata, B. Gong, Y. Seto, A. Takemoto, S. Takagi, H. Ninomiya, N. Yanagitani, M. Nakao, M. Mun, K. Uchibori, M. Nishio, Y. Miyazaki, Y. Shiraishi, S. Ogawa, K. Kataoka, N. Fujita, K. Takeuchi, R. Katayama, Soluble PD-L1 works as a decoy in lung cancer immunotherapy via alternative polyadenylation, JCI Insight 7 (2022) e153323, https://doi.org/10.1172/jci.insight.153323. PMID: 34874919; PMCID: PMC8765052.
[24] N.Z. Malinga, S.C. Siwele, H.C. Steel, L.L.I. Kwofie, P.W.A. Meyer, T. Smit, R. Anderson, B.L. Rapoport, M.C.M. Kgokolo, Systemic levels of the soluble co-inhibitory immune checkpoints, CTLA-4, LAG-3, PD-1/PD-L1 and TIM-3 are markedly increased in basal cell carcinoma, Transl. Oncol. 19 (2022) 101384, https://doi.org/10.1016/j.tranon.2022.101384. PMID: 35255355; PMCID: PMC8898970.
[25] D.I. Gabrilovich, The dawn of myeloid-derived suppressor cells: identification of arginase 1 as the mechanism of immune suppression, Cancer Res 81 (2021) 3953–3955, https://doi.org/10.1158/0008-5472.CAN-21-1237. PMID: 34341063.
[26] E. Puré, R. Blomberg, Pro-tumorigenic roles of fibroblast activation protein in cancer: back to the basics, Oncogene 37 (2018) 4343–4357, https://doi.org/10.1038/s41388-018-0275-3. PMID: 29720723; PMCID: PMC6092565.
[27] A.T. Yang, Y.O. Kim, X.Z. Yan, H. Abe, M. Aslam, K.S. Park, X.Y. Zhao, J.D. Jia, T. Klein, H. You, D. Schuppan, Fibroblast activation protein activates macrophages and promotes parenchymal liver inflammation and fibrosis, Cell Mol. Gastroenterol. Hepatol. 15 (2023) 841–867, https://doi.org/10.1016/j.jcmgh.2022.12.005. PMID: 36521660; PMCID: PMC9972574.
[28] D. Aldinucci, C. Borghese, N. Casagrande, The CCL5/CCR5 axis in cancer progression, Cancers (Basel) 12 (2020) 1765, https://doi.org/10.3390/cancers12071765. PMID: 32630699; PMCID: PMC7407580.
[29] P. Hsu, B. Santner-Nanan, M. Hu, K. Skarratt, C.H. Lee, M. Stormon, M. Wong, S. J. Fuller, R. Nanan, IL-10 potentiates differentiation of human induced regulatory T cells via STAT3 and Foxo1, J. Immunol. 195 (2015) 3665–3674, https://doi.org/10.4049/jimmunol.1402898. PMID: 26363058.
[30] M.J. Polanczyk, E. Walker, D. Haley, B.S. Guerrouahen, E.T. Akporiaye, Blockade of TGF-β signaling to enhance the antitumor response is accompanied by dysregulation of the functional activity of $CD4^+CD25^+Foxp3^+$ and $CD4^+CD25^-Foxp3^+$ T cells, J. Transl. Med. 17 (2019) 219, https://doi.org/10.1186/s12967-019-1967-3. PMID: 31288845; PMCID: PMC6617864.
[31] J.M. Hu, K. Liu, J.H. Liu, X.L. Jiang, X.L. Wang, Y.Z. Chen, S.G. Li, H. Zou, L. J. Pang, C.X. Liu, X.B. Cui, L. Yang, J. Zhao, X.H. Shen, J.F. Jiang, W.H. Liang, X. L. Yuan, F. Li, CD163 as a marker of M2 macrophage, contribute to predict aggressiveness and prognosis of Kazakh esophageal squamous cell carcinoma, Oncotarget 8 (2017) 21526–21538, https://doi.org/10.18632/oncotarget.15630. PMID: 28423526; PMCID: PMC5400603.
[32] A.S.M.R. Haque, M. Moriyama, K. Kubota, N. Ishiguro, M. Sakamoto, A. Chinju, K. Mochizuki, T. Sakamoto, N. Kaneko, R. Munemura, T. Maehara, A. Tanaka, J. N. Hayashida, S. Kawano, T. Kiyoshima, S. Nakamura, CD206+ tumor-associated macrophages promote proliferation and invasion in oral squamous cell carcinoma via EGF production, Sci. Rep. 9 (2019) 14611, https://doi.org/10.1038/s41598-019-51149-1. PMID: 31601953; PMCID: PMC6787225.
[33] M. Sexton, D.B. Jones, M.E. Maloney, Histologic pattern analysis of basal cell carcinoma. Study of a series of 1039 consecutive neoplasms, J. Am. Acad. Dermatol. 23 (1990) 1118–1126, https://doi.org/10.1016/0190-9622(90)70344-h. PMID: 2273112.
[34] R. Pampena, G. Parisi, M. Benati, S. Borsari, M. Lai, G. Paolino, A.M. Cesinaro, S. Ciardo, F. Farnetani, S. Bassoli, G. Argenziano, G. Pellacani, C. Longo, Clinical and dermoscopic factors for the identification of aggressive histologic subtypes of basal cell carcinoma, Front. Oncol. 10 (2021) 630458, https://doi.org/10.3389/fonc.2020.630458. PMID: 33680953; PMCID: PMC7933517.
[35] D.M. Compaan, L.C. Gonzalez, I. Tom, K.M. Loyet, D. Eaton, S.G. Hymowitz, Attenuating lymphocyte activity: the crystal structure of the BTLA-HVEM complex, J. Biol. Chem. 280 (2005) 39553–39561, https://doi.org/10.1074/jbc.M507629200. PMID: 16169851.
[36] J.C. Marie, J.J. Letterio, M. Gavin, A.Y. Rudensky, TGF-β1 maintains suppressor function and Foxp3 expression in $CD4^+CD25^+$ regulatory T cells, J. Exp. Med. 201 (2005) 1061–1067, https://doi.org/10.1084/jem.20042276. PMID: 15809351; PMCID: PMC2213134.
[37] D.A. Vignali, L.W. Collison, C.J. Workman, How regulatory T cells work, Nat. Rev. Immunol. 8 (2008) 523–532, https://doi.org/10.1038/nri2343. PMID: 18566595; PMCID: PMC2665249.
[38] L.M. Francisco, P.T. Sage, A.H. Sharpe, The PD-1 pathway in tolerance and autoimmunity, Immunol. Rev. 236 (2010) 219–242, https://doi.org/10.1111/j.1600-065X.2010.00923.x. PMID: 20636820; PMCID: PMC2919275.
[39] O.S. Qureshi, Y. Zheng, K. Nakamura, K. Attridge, C. Manzotti, E.M. Schmidt, J. Baker, L.E. Jeffery, S. Kaur, Z. Briggs, T.Z. Hou, C.E. Futter, G. Anderson, L. S. Walker, D.M. Sansom, Trans-endocytosis of CD80 and CD86: a molecular basis for the cell-extrinsic function of CTLA-4, Science 332 (2011) 600–603, https://doi.org/10.1126/science.1202947. PMID: 21474713; PMCID: PMC3198051.
[40] J.E. Konkel, D. Zhang, P. Zanvit, C. Chia, T. Zangarle-Murray, W. Jin, S. Wang, W Chen, Transforming growth factor-β signaling in regulatory T cells controls T helper-17 cells and tissue-specific immune responses, Immunity 46 (2017) 660–674, https://doi.org/10.1016/j.immuni.2017.03.015. PMID: 28423340.
[41] T. Maruhashi, D. Sugiura, I.M. Okazaki, T. Okazaki, LAG-3: from molecular functions to clinical applications, J. Immunother. Cancer 8 (2020) e001014, https://doi.org/10.1136/jitc-2020-001014. PMID: 32929051; PMCID: PMC7488795.
[42] M. Tekguc, J.B. Wing, M. Osaki, J. Long, S. Sakaguchi, Treg-expressed CTLA-4 depletes CD80/CD86 by trogocytosis, releasing free PD-L1 on antigen-presenting cells, Proc. Natl. Acad. Sci. U. S. A. 118 (2021) e2023739118, https://doi.org/10.1073/pnas.2023739118. PMID: 34301886; PMCID: PMC8325248.
[43] S. Muth, A. Klaric, M. Radsak, H. Schild, H.C. Probst, CD27 expression on Treg cells limits immune responses against tumors, *J. Mol. Med.* (Berl) 100 (2022) 439–449, https://doi.org/10.1007/s00109-021-02116-9. PMID: 34423375; PMCID: PMC8843905.
[44] L. Vence, S.L. Bucktrout, I. Fernandez Curbelo, J. Blando, B.M. Smith, A.E. Mahne, J.C. Lin, T. Park, E. Pascua, T. Sai, J. Chaparro-Riggers, S.K. Subudhi, J.B. Scutti, M.G. Higa, H. Zhao, S.S. Yadav, A. Maitra, I.I. Wistuba, J.P. Allison, P Sharma, Characterization and comparison of GITR expression in solid tumors, Clin. Cancer Res. 25 (2019) 6501–6510, https://doi.org/10.1158/1078-0432.CCR-19-0289. PMID: 31358539; PMCID: PMC6825542.
[45] A. Pedroza-Gonzalez, G. Zhou, S.P. Singh, P.P. Boor, Q. Pan, D. Grunhagen, J. de Jonge, T.K. Tran, C. Verhoef, J.N. IJzermans, H. Janssen, K. Biermann, J. Kwekkeboom, D. Sprengers, GITR engagement in combination with CTLA-4 blockade completely abrogates immunosuppression mediated by human liver tumor-derived regulatory T cells *ex vivo*, Oncoimmunology 4 (2015) e1051297, https://doi.org/10.1080/2162402X.2015.1051297. PMID: 26587321; PMCID: PMC4635937.
[46] S. Rachidi, A. Metelli, B. Riesenberg, B.X. Wu, M.H. Nelson, C. Wallace, C. M. Paulos, M.P. Rubinstein, E. Garrett-Mayer, M. Hennig, D.W. Bearden, Y. Yang, B. Liu, Z. Li, Platelets subvert T cell immunity against cancer via GARP-TGFβ axis, Sci. Immunol. 2 (2017) eaai7911, https://doi.org/10.1126/sciimmunol.aai7911. PMID: 28763790; PMCID: PMC5539882.
[47] G. de Streel, C. Bertrand, N. Chalon, S. Liénart, O. Bricard, S. Lecomte, J. Devreux, M. Gaignage, G. De Boeck, L. Mariën, I. Van De Walle, B. van der Woning, M. Saunders, H. de Haard, E. Vermeersch, W. Maes, H. Deckmyn, P.G. Coulie, N. van Baren, S. Lucas, Selective inhibition of TGF-β1 produced by GARP-expressing Tregs overcomes resistance to PD-1/PD-L1 blockade in cancer, Nat. Commun. 11 (2020) 4545, https://doi.org/10.1038/s41467-020-17811-3. PMID: 32917858; PMCID: PMC7486376.
[48] A. Metelli, M. Salem, C.H. Wallace, B.X. Wu, A. Li, X. Li, Z Li, Immunoregulatory functions and the therapeutic implications of GARP-TGF-β in inflammation and cancer, J. Hematol. Oncol. 11 (2018) 24, https://doi.org/10.1186/s13045-018-0570-z. PMID: 29458436; PMCID: PMC5819195.
[49] S. Lecomte, J. Devreux, G. de Streel, N. van Baren, V. Havelange, D. Schröder, N. Vaherto, C. Vanhaver, C. Vanderaa, N. Dupuis, C. Pecquet, P.G. Coulie, S. N. Constantinescu, S. Lucas, Therapeutic activity of GARP:tGF-β1 blockade in murine primary myelofibrosis, Blood 141 (2023) 490–502, https://doi.org/10.1182/blood.2022017097. PMID: 36322928.
[50] D. Peng, M. Fu, M. Wang, Y. Wei, X Wei, Targeting TGF-β signal transduction for fibrosis and cancer therapy, Mol. Cancer 21 (2022) 104, https://doi.org/10.1186/s12943-022-01569-x. PMID: 35461253; PMCID: PMC9033932.
[51] J.H. Kang, M.Y. Jung, M. Choudhury, E.B. Leof, Transforming growth factor beta induces fibroblasts to express and release the immunomodulatory protein PD-L1 into extracellular vesicles, FASEB J 34 (2020) 2213–2226, https://doi.org/10.1096/fj.201902354R. PMID: 31907984.
[52] H.W. Rogers, M.A. Weinstock, S.R. Feldman, B.M. Coldiron, Incidence estimate of nonmelanoma skin cancer (Keratinocyte Carcinomas) in the U.S. Population, JAMA Dermatol 2015 (151) (2012) 1081–1086, https://doi.org/10.1001/jamadermatol.2015.1187. PMID: 25928283.
[53] M.S. Heath, A. Bar, Basal cell carcinoma, Dermatol. Clin. 41 (2023) 13–21, https://doi.org/10.1016/j.det.2022.07.005. PMID: 36410973.
[54] E.V. Di Brizzi, G. Argenziano, G. Brancaccio, C. Scharf, A. Ronchi, E. Moscarella, The current clinical approach to difficult-to-treat basal cell carcinomas, Expert Rev. Anticancer Ther. 23 (2023) 43–56, https://doi.org/10.1080/14737140.2023.2161517. PMID: 36579630.

[55] K. Peris, M.C. Fargnoli, C. Garbe, R. Kaufmann, L. Bastholt, N.B. Seguin, V. Bataille, V.D. Marmol, R. Dummer, C.A. Harwood, A. Hauschild, C. Höller, M. Haedersdal, J. Malvehy, M.R. Middleton, C.A. Morton, E. Nagore, A.J. Stratigos, R.M. Szeimies, L. Tagliaferri, M. Trakatelli, I. Zalaudek, A. Eggermont, J.J. Grob, European Dermatology Forum (EDF), the European Association of Dermato-Oncology (EADO) and the European Organization for Research and Treatment of Cancer (EORTC). Diagnosis and treatment of basal cell carcinoma: european consensus-based interdisciplinary guidelines, Eur. J. Cancer 118 (2019) 10–34, https://doi.org/10.1016/j.ejca.2019.06.003. PMID: 31288208.

[56] E.J. Lipson, M.T. Lilo, A. Ogurtsova, J. Esandrio, H. Xu, P. Brothers, M. Schollenberger, W.H. Sharfman, J.M. Taube, Basal cell carcinoma: PD-L1/PD-1 checkpoint expression and tumor regression after PD-1 blockade, J. Immunother. Cancer 5 (2017) 23, https://doi.org/10.1186/s40425-017-0228-3. PMID: 28344809; PMCID: PMC5360064.

[57] A.J. Stratigos, A. Sekulic, K. Peris, O. Bechter, S. Prey, M. Kaatz, K.D. Lewis, N. Basset-Seguin, A.L.S. Chang, S. Dalle, A.F. Orland, L. Licitra, C. Robert, C. Ulrich, A. Hauschild, M.R. Migden, R. Dummer, S. Li, S.Y. Yoo, K. Mohan, E. Coates, V. Jankovic, N. Fiaschi, E. Okoye, I.D. Bassukas, C. Loquai, V. De Giorgi, Z. Eroglu, R. Gutzmer, J. Ulrich, S. Puig, F. Seebach, G. Thurston, D.M. Weinreich, G.D. Yancopoulos, I. Lowy, T. Bowler, M.G. Fury, Cemiplimab in locally advanced basal cell carcinoma after hedgehog inhibitor therapy: an open-label, multi-centre, single-arm, phase 2 trial, Lancet Oncol 22 (2021) 848–857, https://doi.org/10.1016/S1470-2045(21)00126-1. PMID: 34000246.

[58] FDA (U.S. Food & Drug Administration). FDA approves cemiplimab-rwlc for locally advanced and metastatic basal cell carcinoma. Content current as of: 02/09/2021. Last accessed on the 10th April 2023. https://www.fda.gov/drugs/resources-information-approved-drugs/fda-approvescemiplimab-rwlc-locally-advanced-andmetastatic-basal-cell-carcinoma.

[59] Libtayo®, Cemiplimab) approved by the European Commission as the first immunotherapy indicated for patients with advanced basal cell carcinoma, BioSpace (June 25, 2021). Accessed 10th April 2023, https://www.biospace.com/article/libtayocemiplimab-approved-by-the-european-commission-as-the-first-immunotherapyindicatedfor-patients-with-advanced-basal-cell-carcinoma/.

[60] T. Damsin, E. Lebas, N. Marchal, A. Rorive, Nikkels AF. Cemiplimab for locally advanced and metastatic basal cell carcinoma, Expert Rev. Anticancer Ther. 22 (2022) 243–248, https://doi.org/10.1080/14737140.2022.2043748. PMID: 35175882.

[61] C.G. Graydon, S. Mohideen, K.R. Fowke, LAG3's enigmatic mechanism of action, Front. Immunol. 11 (2021) 615317, https://doi.org/10.3389/fimmu.2020.615317. PMID: 33488626; PMCID: PMC7820757.

[62] Y. Wolf, A.C. Anderson, V.K. Kuchroo, TIM3 comes of age as an inhibitory receptor, Nat. Rev. Immunol. 20 (2020) 173–185, https://doi.org/10.1038/s41577-019-0224-6. PMID: 31676858; PMCID: PMC7327798.

[63] L.K. Huynh, C.J. Hipolito, Ten Dijke P. A perspective on the development of TGF-β inhibitors for cancer treatment, Biomolecules 9 (2019) 743, https://doi.org/10.3390/biom9110743. PMID: 31744193; PMCID: PMC6921009.

[64] C.H. Jin, M. Krishnaiah, D. Sreenu, V.B. Subrahmanyam, K.S. Rao, H.J. Lee, S. J. Park, H.J. Park, K. Lee, Y.Y. Sheen, D.K. Kim, Discovery of N-((4-([1,2,4]triazolo [1,5-*a*]pyridin-6-yl)-5-(6-methylpyridin-2-yl)-1H-imidazol-2-yl)methyl)-2-fluoroaniline (EW-7197): a highly potent, selective, and orally bioavailable inhibitor of TGF-β type I receptor kinase as cancer immunotherapeutic/antifibrotic agent, J. Med. Chem. 57 (2014) 4213–4238, https://doi.org/10.1021/jm500115w. PMID: 24786585.

[65] S. Herbertz, J.S. Sawyer, A.J. Stauber, I. Gueorguieva, K.E. Driscoll, S.T. Estrem, A. L. Cleverly, D. Desaiah, S.C. Guba, K.A. Benhadji, C.A. Slapak, M.M. Lahn, Clinical development of galunisertib (LY2157299 monohydrate), a small molecule inhibitor of transforming growth factor-beta signaling pathway, Drug Des. Devel. Ther. 9 (2015) 4479–4499, https://doi.org/10.2147/DDDT.S86621. PMID: 26309397; PMCID: PMC4539082.

[66] J. Strauss, C.R. Heery, J. Schlom, R.A. Madan, L. Cao, Z. Kang, E. Lamping, J. L. Marté, R.N. Donahue, I. Grenga, L. Cordes, O. Christensen, L. Mahnke, C. Helwig, J.L. Gulley, Phase I trial of M7824 (MSB0011359C), a bifunctional fusion protein targeting PD-L1 and TGFβ, in advanced solid tumors, Clin. Cancer Res. 24 (2018) 1287–1295, https://doi.org/10.1158/1078-0432.CCR-17-2653. PMID: 29298798; PMCID: PMC7985967.

[67] M.J. Birrer, L.R. Mileshkin, K. Fujiwara, I. Ray-Coquard, J. Alexandre, A. Okamoto, M.R. Mirza, J.L. Gulley, G. Jehl, S. Ramage, L.S. Ojalvo, S.M. Campos, Abstract 879TiP: phase II study of bintrafusp alfa, a bifunctional fusion protein targeting TGF-β and PD-L1, in platinum-experienced advanced cervical cancer, Ann. Oncol. 31 (Suppl 4) (2020) S644–S645, https://doi.org/10.1016/j.annonc.2020.08.1018.

[68] H.G. Kaporis, E. Guttman-Yassky, M.A. Lowes, A.S. Haider, J. Fuentes-Duculan, K. Darabi, J. Whynot-Ertelt, A. Khatcherian, I. Cardinale, I. Novitskaya, J. G. Krueger, J.A. Carucci, Human basal cell carcinoma is associated with Foxp3$^{+}$ T cells in a Th2 dominant microenvironment, J. Invest. Dermatol. 127 (2007) 2391–2398, https://doi.org/10.1038/sj.jid.5700884. PMID: 17508019.

[69] S.H. Omland, P.S. Nielsen, L.M. Gjerdrum, R. Gniadecki, Immunosuppressive environment in basal cell carcinoma: the role of regulatory T cells, Acta. Derm. Venereol. 96 (2016) 917–921, https://doi.org/10.2340/00015555-2440. PMID: 27117439.

[70] P. Ferronika, S.A. Dhiyani, T. Budiarti, I. Widodo, H.T. Rinonce, S.L. Anwar Regulatory T cells but not tumour-infiltrating lymphocytes correlate with tumour invasion depth in basal cell carcinoma. Diagnostics (Basel) 2022, 12, 2987. 10.3390/diagnostics12122987. PMID: 36552993; PMCID: PMC9776706.

[71] J. van den Bulk, N.F.C.C. de Miranda, Ten Dijke P. Therapeutic targeting of TGF-β in cancer: hacking a master switch of immune suppression, Clin. Sci. 135 (2021) 35–52, https://doi.org/10.1042/CS20201236. PMID: 33399850; PMCID: PMC7796313.